Effects of pacing magnitudes and forms on bistability width in a modeled ventricular tissue

Xiaodong Huang,[1,*] Xuemei Liu,[1] Lixian Zheng,[1] Yuanyuan Mi,[2] and Yu Qian[3,†]
[1]*Department of Physics, South China University of Technology, Guangzhou 510640, China*
[2]*Center for Systems Biology, Soochow University, Suzhou 215006, China*
[3]*Nonlinear Research Institute, Baoji University of Arts and Sciences, Baoji 721007, China*
(Received 5 March 2013; revised manuscript received 16 June 2013; published 11 July 2013)

Bistability in periodically paced cardiac tissue is relevant to cardiac arrhythmias and its control. In the present paper, one-dimensional tissue of the phase I Luo-Rudy model is numerically investigated. The effects of various parameters of pacing signals on bistability width are studied. The following conclusions are obtained: (i) Pacing can be classified into two types: pulsatile and sinusoidal types. Pulsatile pacing reduces bistability width as its magnitude is increased. Sinusoidal pacing increases the width as its amplitude is increased. (ii) In a pacing period the hyperpolarizing part plays a more important role than the depolarizing part. Variations of the hyperpolarizing ratio in a period evidently change the width of bistability and its variation tendency. (iii) A dynamical mechanism is proposed to qualitatively explain the phenomena, which reveals the reason for the different effects of pulsatile and sinusoidal pacing on bistability. The methods for changing bistability width by external pacing may help control arrhythmias in cardiology.

DOI: 10.1103/PhysRevE.88.012711 PACS number(s): 87.19.Hh, 05.45.−a

I. INTRODUCTION

Cardiac arrhythmias are diseases with a prevalence in human beings, among which ventricular fibrillation may cause sudden death without immediate treatment [1]. Investigations from the viewpoint of physics promote the research of cardiac diseases [2–9]. The interpretations of dynamical properties of cardiac activities may help to develop safe and effective therapeutic methods for arrthymias [10–13]. Therefore, the interdiscipline of cardiovascular physics is expected to contribute more to cardiology.

In the present paper we intend to investigate bistability in a modeled periodically paced ventricular tissue by physical analysis. Bistability in the ventricle was reported by Mines [14] experimentally. Moreover, various kinds of bistability were found *in vivo* in hearts and cardiac models, which indicates that bistability is prevalent in cardiac systems [15–25]. In periodically paced ventricular tissue, bistability means that the ventricle responds to the pacing by two possible patterns (e.g., 1:1 and 2:1 patterns) in a certain range of stimulation frequency. Generally speaking, two issues about this kind of bistability are mainly concerned: the ionic mechanisms [21,24,25] and the nonlinear dynamics of the mapping models [19,20,22–24]. In Ref. [26] a physical mechanism analyzing the interactive dynamics of pacing period and action potential duration (APD) is proposed.

Bistability is relevant to arrhythmias and its control. It was pointed out that the existence of bistability in ventricles may cause the breakup of spiral waves and thus the emergence of fibrillations [27]. On the other hand, bistability may affect the control of spiral waves. There is a theoretically harmless and effective method to eliminate spiral waves in ventricular tissue [12,28]. The idea is to produce regularly propagating waves by local pacing with a higher frequency than that of the spirals, and the spirals may be driven out. However, due to the existence of bistability, the propagating waves may respond to pacing in a 2:1 state with a frequency lower than that of the spirals, and control is considered to fail. But note that under identical conditions a larger frequency can be obtained on the 1:1 branch and control may succeed [26]. Therefore, the range of bistability (it is called bistability width in the following text) is a quantity determining the robustness of bistability, which affects the occurrence and control of arrhythmias. Understanding how large and how to vary bistability width in periodically paced ventricular tissue is a significant problem.

It is revealed that physiological parameters have influences on the form and width of bistability [24,26]. Also the pacing magnitude has influences on bistability behaviors of a single cell [24]. However, the effects of the pacing parameters on bistability in tissue have not been sufficiently evaluated.

In the present paper, influences of the pacing parameters on bistability width is studied. It is surprising that pacing parameters have great effects on bistability width. As pacing magnitude is increased, the variation tendencies of width under pulsatile and sinusoidal pacing are opposite. A possible analytical theory is proposed to explain the phenomena qualitatively. In a practical situation, physiological conditions are difficult to change (or to change in a slow process [29]), while the external pacing can be easily controlled. It is hoped that our work may provide theoretically reasonable and practical methods for modulating bistability width.

In the present study, a one-dimensional (1D) phase I Luo-Rudy model (LRd91) [30] is numerically investigated. The paper is organized as follows: Section II introduces the model and methods. Section III shows the influences of the pacing parameters on the bistability width. The mechanism of the phenomena is discussed in Sec. IV. The last section is our summary.

II. MODEL AND METHODS

The partial differential equation for the dynamics of the cell's membrane potential V_m (mV) in a 1D tissue is

$$\frac{\partial V_m(x,t)}{\partial t} = \frac{-I_{ion} + I_{st}(x,t)}{C_m} + D\nabla^2 V_m(x,t), \qquad (1)$$

*schuangxd@scut.edu.cn
†qianyu0272@163.com

where $C_m = 1\mu\text{F/cm}^2$ is the membrane capacitance, $D = 0.001\ \text{cm}^2/\text{ms}$ is the diffusion coefficient, I_{ion} ($\mu\text{A/cm}^2$) is the total transmembrane ionic current of a cell, and I_{st} ($\mu\text{A/cm}^2$) is the stimulating current. In the LRd91 model, the total ionic current I_{ion} is the summary of six individual ionic currents:

$$I_{ion} = I_{Na} + I_{si} + I_K + I_{K1} + I_{Kp} + I_b, \tag{2}$$

where $I_{Na} = G_{Na}m^3hj(V_m - E_{Na})$, $I_{si} = G_{si}df(V_m - E_{si})$, $I_K = G_K XX_i(V_m - E_K)$, $I_{K1} = G_{K1}K1_\infty(V_m - E_{K1})$, $I_{Kp} = G_{Kp}Kp(V_m - E_{Kp})$, $I_b = G_b(V_m - E_b)$. Here m, h, j, d, f, and X are gating variables and the evolvement of each of them satisfies

$$\frac{dy}{dt} = \frac{y_\infty - y}{\tau_y}, \tag{3}$$

where y represents any gating variable, τ_y and y_∞ are the time constant and the steady state of y, respectively. The detailed description of this model was given by Luo and Rudy [30].

For numerical simulation, Eq. (1) is integrated by the explicit Euler method. Moreover, some other numerical methods are often used to simulate cardiac models [8,31]. In the present work, time step $dt = 0.02$ ms and space step $dx = 0.028$ cm are chosen. The 1D chain consists of 200 nodes. The gating variable equations are solved by the Rush-Larsen method [32]. The pacing is applied on the leftmost cell of the cable and the no-flux boundary condition is used. The numerical errors of the method and spatiotemporal resolution are estimated in the Appendix. All parameters are set to be the same as the original LRd91 model except $G_{si} = 0.055\ \text{mS/cm}^2$ and $G_K = 0.705\ \text{mS/cm}^2$. This set of parameters reduces the slope of APD restitution curve and excludes alternans (the so called 2:2 rhythm) in the distant region of the cable. Under such a condition, the bistability window is formed between 1:1 and 2:1, which is a typical kind of bistability found in cardiac tissue [23]. On the other hand, the bistability window has a large enough width, so that the characteristics of the variations could be easily observed.

Bistability is depicted by bifurcation diagram of action potential duration (APD) vs pacing cycle length (PCL). Action potential duration is defined as the time to reach the fixed transmembrane voltage $V_m = -62$ mV in an action potential. For each PCL, data of the first 100 times of pacing are discarded and the following 20 times are recorded. Data of entrainment are collected from the 150th grid-point counting from the paced end unless specified otherwise. When PCL is changed downward and upward (by 1 ms for each step) in a loop continuously (the final state of the cable at the present PCL is the initial state for the next one), bistability can be formed in the bifurcation diagram.

Figure 1 is a bistability window shown in the PCL-APD diagram. The boundaries of the window are defined as follows. The left boundary is at the point that PCL equals $\text{PCL}_{2:1b}$ (labeled by the arrow on the left in Fig. 1). This point is obtained by decreasing PCL continuously on the 1:1 branch until a steady 2:1 state is reached. The right boundary is at PCL equaling $\text{PCL}_{1:1b}$ (labeled by the arrow on the right in Fig. 1). This point is obtained by increasing PCL continuously on the 2:1 branch until a steady 1:1 state is reached. Then the width of the window W (ms) is $W = T_{p_{1:1b}} - T_{p_{2:1b}}$ (T_p is used to denote the value of PCL in mathematical expression in the following text). For each set of pacing parameters, the above process is repeated to obtain an integral bistability window. The width W corresponding to the parameter set is measured from the window.

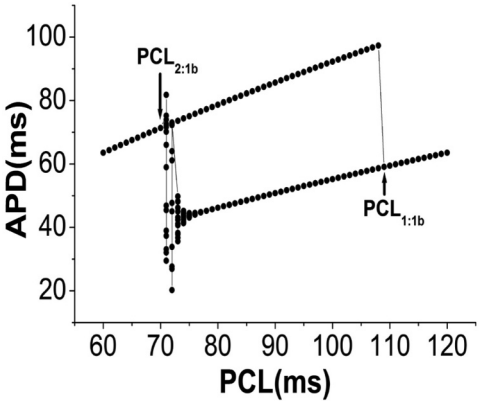

FIG. 1. Bistability window in 1D cardiac tissue. Pulsatile pacing with duration of 10 ms and magnitude 30($\mu\text{A/cm}^2$) is applied on the left end. Data in the diagram are measured from the 150th cell counting from the pacing end. The first 100 times of pacing is discarded. The values of PCL labeled $\text{PCL}_{2:1b}$ and $\text{PCL}_{1:1b}$ are defined to be the boundaries of the window.

III. EFFECTS OF PACING MAGNITUDES AND FORMS ON BISTABILITY IN TISSUE

In this section the effects of the pacing parameters on the width W is investigated. The two regularly used kinds of pacing forms, pulsatile and sinusoidal forms, are considered. Interestingly, in the pulsatile pacing form W decreases as the pacing magnitude is increased [as shown in Fig. 2(a) by black solid circles], while in sinusoidal pacing form W increases as the pacing amplitude is increased [as shown in Fig. 2(a) by red empty circles]. The variations of the width show opposite tendencies under the two different forms of pacing. The variations of W are not smooth, and "increase" or "decrease" is used to describe the overall variation tendency. The fluctuations may be partly due to the irregular region between the stable 1:1 and 2:1 states on the left of the bistability window (as shown in Fig. 1), which is caused by complex dynamics of propagation block in the cable [33–35]. Moreover, the fluctuations are also relevant to the artifacts of numerical result. Sometimes 100 times of pacing are not enough for eliminating the transient effect, and the position of the 1:1→2:1 transition is not detected precisely. So that the range of the region may vary irregularly by 1–2 ms for different pacing magnitudes. However, the fluctuations do not imperil the conclusions. For simplicity of presentation in the paper, the fluctuations are ignored and the words "increase" and "decrease" are used.

For a cardiac cell, depolarizing current and hyperpolarizing current have different effects on cell dynamics [36,37]. The obvious difference between pulsatile and sinusoidal pacing is that sinusoidal pacing possesses a hyperpolarizing part but pulsatile pacing does not. Thus hyperpolarizing stimulation may be the reason for the opposite tendencies. Based on the above consideration, we do further investigations as follows:

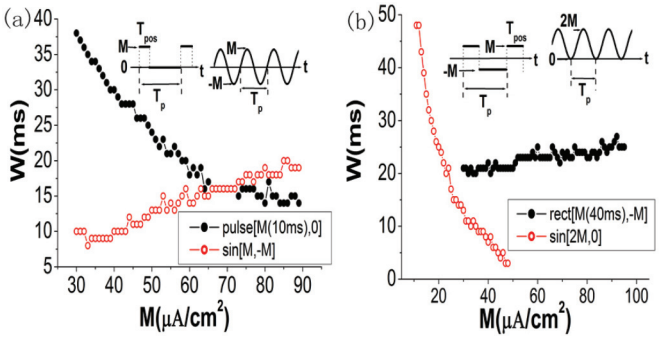

FIG. 2. (Color online) Bistability window width varied by increasing magnitudes of pulsatile and sinusoidal pacing. Pacing forms are shown in the top of the panels. (a) Situations of pulsatile and sinusoidal pacing. The duration of pulse (represented by T_{pos}) is 10 ms. For pulsatile form the width is decreased by the increase of the magnitude (shown by black solid circles), while for sinusoidal form it is increased by the increase of the amplitude (shown by red empty circles). (b) Situations of rectangular and shifted sinusoidal pacing. In rectangular form duration of the positive stimulation is $T_{pos} = 40$ ms. The sinusoidal signal is wholly shifted by M so that the negative part is eliminated. Interestingly, the variation tendency of width increases under rectangular form and decreases under shifted sinusoidal form.

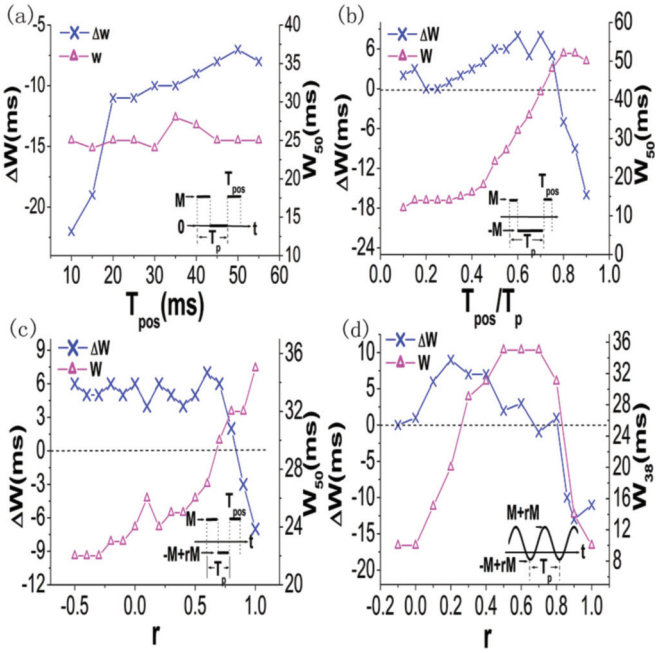

FIG. 3. (Color online) The influences of pacing parameters on bistability width. Pacing signals varied are shown in each panel. ΔW describes the variation tendency as magnitude is increased for a given form of pacing, and $\Delta W > 0$ means the variation tendency is ascending while < 0 means descending. W_M roughly positions the M-W curve. (a) The effect of depolarizing part of pulsatile pacing (represented by variations of T_{pos}). (b) The effect of the ratio of T_{pos} to pacing period T_p in rectangular pacing. For example, $T_{pos}/T_p = 0.5$ means the functioning time range of positive M is kept to be $0.5T_p$ during PCL is changed in a loop. (c) The effect of r in rectangular form, which determines the relative value of positive and negative magnitudes. For example, $r = 0.4$ means the negative magnitude is 0.4 times less than the positive one. T_{pos} is $0.5T_p$ during changing r. (d) The effect of the shifted degree of sinusoidal signal (represented by r). From the four pictures it can be seen that hyperpolarizing part plays a much more important role in varying the bistability width. Increase of hyperpolarizing ratio transforms the pacing type from pulsatile to sinusoidal [see blue crosses in (c) and (d) moving from below to above 0], and evidently reduces W_M [see pink empty triangles in (c) and (d) descending as T_{pos}/T_p and r are decreased], which means evident downward shift of the M-W curve. However, change of depolarizing ratio does not have the effect.

(i) The sinusoidal pacing is changed to $I_{st} = M\sin\omega t + M$ so that the hyperpolarizing effect is eliminated. (ii) The pulsatile pacing is changed to rectangular form so that it possesses a hyperpolarizing part, i.e., $I_{st} = M$ [mod$(T,T_p) \leqslant T_{pos}$]; $I_{st} = -M$ [mod$(T,T_p) > T_{pos}$], where M is the magnitude, T_p is the pacing period (T_p equals PCL) and T_{pos} is the time range for which the stimulation magnitude is positive M. The influences of magnitude on width in the two modified cases are shown in Fig. 2(b). We can see that pacing without the hyperpolarizing part [the red empty circles in Fig. 2(b)] has a similar effect to the pulsatile form [the black solid circles in Fig. 2(a)], while pacing with the hyperpolarizing part [the black solid circles in Fig. 2(b)] has a similar effect to the sinusoidal form [the red empty circles in Fig. 2(a)]. Therefore, the variation tendency of W depends on the magnitudes of the depolarizing and hyperpolarizing parts instead of pacing forms.

Besides the magnitude M, there are still multiple parameters of pacing, which change the pacing form. The parameters in the two kinds of pacing are presented by the following symbols: (i) $R[M(T_{pos}), -M + rM]$, which means the pacing form is rectangular, M is the positive magnitude and $-M + rM$ is the negative magnitude, T_{pos} is the functioning time range of positive M in a period, and r determines the relative value between the positive and negative magnitudes; (ii) $S[M + rM, -M + rM]$, which means the pacing is sinusoidal, and M is the amplitude. As the shape of the sinusoidal curve is fixed, only the parameter determining the upwards and downwards shifting extents of the whole curve is changed, which is determined by r.

Our ideas for investigating the effects of the parameters are as follows. Each set of T_{pos} and r determines the form of pacing. For a given form of pacing, the effect of M on bistability width is shown in the M-W coordinate (just like Fig. 2). When T_{pos} and r are changed, the M-W curve will be changed correspondingly. It is impossible to figure out all the curves with each set of pacing parameters. Therefore, variations of the M-W curve are described by the following two quantities for simplicity: ΔW and W_M. The quantity ΔW is the difference between W_{M_1} and W_{M_2} ($\Delta W = W_{M_2} - W_{M_1}$). For R form pacing $M_1 = 30$ and $M_2 = 80$, and for S form pacing $M_1 = 28$ and $M_2 = 48$. ΔW describes the variation tendency of the width as the magnitude M is increased ($\Delta W > 0$ means ascending and $\Delta W < 0$ means descending). Another quantity W_M is the width of a certain M ($M = 50$ for the R form and $M = 38$ for the S form), which can roughly position the curve in the M-W plane.

Figure 3 shows the effects of the pacing parameters. We discuss three problems by this figure as follows:

(i) Classification of the pacing forms. According to the variation tendency of W, the pacing forms can be classified into two types: the sinusoidal type and the pulsatile type. Pacing forms that give $\Delta W \geqslant 0$ are regarded to be the sinusoidal type because they have a similar effect to the normal sinusoidal pacing. The sinusoidal type increases bistability width as its amplitude is increased [$\Delta W \geqslant 0$, as shown by the blue crosses in Fig. 3(b) with $T_{pos} \leqslant 0.75T_p$, Fig. 3(c) with $r \leqslant 0.8$, and Fig. 3(d) with $r \leqslant 0.8$]. The characteristic of the sinusoidal type is that hyperpolarizing part occupies a certain degree in the pacing. Pacing forms that give $\Delta W < 0$ are regarded to be the pulsatile type because they have a similar effect to the normal pulsatile pacing. The pulsatile type decreases the width as its magnitude is increased [$\Delta W < 0$, as shown by blue crosses in Fig. 3(a), Fig. 3(b) with $T_{pos} \geqslant 0.8T_p$, Fig. 3(c) with $r \geqslant 0.9$, and Fig. 3(d) with $r \geqslant 0.9$]. The characteristic of this type is that the depolarizing part takes absolute advantage over the hyperpolarizing one.

(ii) Effects of depolarizing part in the pacing. In pulsatile pacing, the variation of the depolarizing part ratio in a pacing period (represented by T_{pos}) changes W_{50} scarcely, and reduces $|\Delta W|$ as its ratio is increased in a period [Fig. 3(a)]. That means that an increase of the depolarizing part in pulsatile pacing will flatten the M-W curve, and will hold the curve in an approximately invariant position.

(iii) Effects of hyperpolarizing part. When the hyperpolarizing part appears in the pulsatile pacing with a very small and increased ratio [decreased T_{pos}/T_p and r mean an increased ratio of the hyperpolarizing part in Figs. 3(b)–3(d)], it greatly reduces $|\Delta W|$ [see the blue crosses below 0 in Figs. 3(b)–3(d), which move towards 0]. When the ratio becomes larger, ΔW becomes positive and the pacing transforms to the sinusoidal type [see the blue crosses above 0 in Figs. 3(b)–3(d)]. On the other hand, variations of the hyperpolarizing ratio evidently change W_M. The quantity increases as the hyperpolarizing ratio is decreased [as shown in Figs. 3(b)–3(d) by pink empty triangles]. But in sinusoidal pacing, when $r \geqslant 0.8$, W_M becomes decreased. However, in a large range of parameters the above conclusion is held.

From the above discussions, it can be seen that changes of hyperpolarizing ratio in a pacing period may transform the pacing type between pulsatile and sinusoidal types and evidently change the bistability width. But the depolarizing part does not possess the ability. In conclusion, the hyperpolarizing part influences bistability width in a much greater degree than the depolarizing one. The results in the present section may provide effective ways to adjust bistability width by varying pacing parameters.

IV. THEORETICAL EXPLANATION OF THE PHENOMENA

In this section we want to qualitatively explain the contrary tendencies of width variation under pulsatile and sinusoidal pacing [the phenomena shown by Fig. 2(a)].

Figure 4(a) shows two bistability windows under an identical form of pacing with different magnitudes. It can be seen that the left boundaries of the windows are nearly at the identical PCL, and the difference of the width comes from the right boundaries. Figure 4(b) shows the spatiotemporal

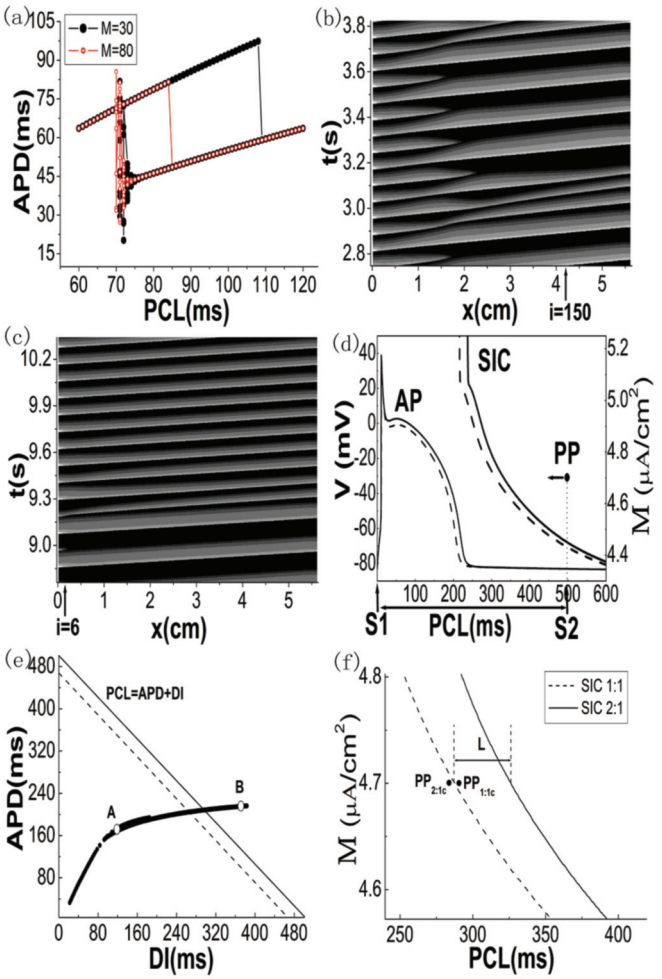

FIG. 4. (Color online) Dynamical mechanisms of bistability in tissue and a single cell. (a) Bistability windows produced by pulsatile pacing with $T_{pos} = 10$ ms. The window made up of black solid circles and red empty circles are produced by $M = 30(\mu$ A/cm$^2)$ and $80(\mu$A/cm$^2)$, respectively. The width difference is mainly due to the difference of the right boundaries. (b) Spatiotemporal pattern of 1:1 lost. The pacing period is 72 ms. Synchronization of 1:1 is lost in the distant region and 1:1 is approximately held in the adjacent cells. (c) Spatiotemporal pattern of 1:1 recovery from 2:1 (PCL is varied from 108 to 109 ms). The whole cable follows the adjacent cells to fall in 1:1. (d) Dynamical process of APD and SIC when PCL is decreased. The process is as follows: PP moves leftward→APD reduces→SIC moves leftward. (e) DAPDRC of a paced single cell. As PCL is decreased, the solid line representing $T_p = A + D$ moves downward, and APD is reduced. When 1:1 transforms to be 2:1, APD is enlarged (point A jumps to point B). (f) SIC movement when 2:1 is reached. Corresponding to APD enlargement, SIC jumps from the dashed position to the solid one with a distance L.

pattern of the critical state that 1:1 is lost. It reveals that desynchronization of 1:1 is due to the propagation block in the region distant from the paced end, and is irrelevant to pacing magnitude, so that the left boundaries of the two bistability windows shown in Fig. 4(a) coincide with each other. Figure 4(c) shows the transition from stable 2:1 to 1:1. It reveals that if 1:1 is recovered on the cells adjacent to the paced end, it would also be recovered on the whole cable. Therefore, the differences of width under different magnitudes

is determined by the dynamics of cells adjacent to the paced end rather than the distant ones.

Additionally, in regard to the wave propagation block shown in Fig. 4(b), a number of works have discussed its mechanisms in detail [33–35]. When the APD of a certain cell in the cable is too large and pacing is fast, the following stimulus will meet the refractory period and fail to excite the cell, and propagation is blocked at this site. The previous studies revealed that propagation block is associated to three factors: dispersion of velocity (represented by CV restitution curve), APD restitution property (represented by APD restitution curve), and coupling strength of the cable. The irregular region in the bistability window shown in Fig. 4(a) is partly due to the complex dynamics of propagation blocks, the width of which may fluctuate by 1–2 ms irregularly.

Based on the above findings, it can be concluded that the bistability dynamics of the adjacent cells roughly determine that of the whole tissue. In this section, the sixth cell is selected to investigate the mechanism of width variation. But note that investigations on another adjacent cell (such as the fifth, fourth, etc.) provide similar results.

A. Mechanism of bistability in a single cell

In Ref. [26] a dynamical mechanism of bistability between 1:1 and 2:1 in a single periodically paced cardiac cell is proposed. The theory will be applied to investigate bistability width in our work. In this subsection a brief review of the mechanism is given.

Pulsatile pacing is usually applied and the results in this subsection are founded on this type of pacing. Figures 4(d)–4(f) are schematic diagrams showing the mechanism. In Fig. 4(d) the solid curve labeled AP (action potential) is the transmembrane potential elicited by one time of stimulation in the pacing (labeled S1). The solid disk labeled PP (pacing point) represents the stimulus following S1 (labeled S2) with time interval S1S2 equal to PCL and a certain magnitude. The solid curve labeled SIC (strength-interval curve), corresponding to the solid AP, indicates the minimum magnitude of S2 needed to elicit another AP at certain time intervals following S1 [38]. If the PP is above SIC, 1:1 could be obtained, while below SIC 1:1 would be lost and 2:1 takes place. Here the vulnerable window [6,37] is not considered, because the mechanism of bistability depends on the relative positions of PP and SIC, and the vulnerable window has little influence on the results.

When the PCL is decreased [the PP moves leftward, indicated by a left pointed arrow in Fig. 4(d)], the APD is reduced. Such a variation is shown by Fig. 4(e), which is the so called dynamic APD restitution curve (DAPDRC) [4,19]. The steady 1:1 state is represented by the intersection point of the DAPDRC and the solid straight line representing $T_p = A + D$ [A and D mean the values of the APD and the DI (diastolic interval) in a mathematical expression]. Therefore, when the PCL is decreased, the solid straight line in Fig. 4(e) moves to the position of the dashed one, and the APD is reduced. Correspondingly, in Fig. 4(d) the AP curve shrinks to be the dashed one, and the SIC moves leftward to be the dashed one as a result. The dynamical process is as follows: PP moves leftward→APD reduces→SIC moves leftward.

The moving velocity of the SIC is determined by the varying rate of the APD. Note that the PP moves faster than the SIC when the PCL is changed (the variation of the APD is smaller than that of the PCL). When the PP goes leftward and locates below the SIC [see Fig. 4(f); $PP_{1:1c}$ moves left to the position of $PP_{2:1c}$, and goes under the dashed SIC], 1:1 is lost. In the 2:1 state the actual excitation period is 2PCL. As indicated by DAPDRC in Fig. 4(e), the APD of the 2:1 state (represented by point B) is larger than the 1:1 state (represented by point A). Therefore, when the 2:1 entrainment is reached, the APD enlarges and the SIC jumps rightward by a certain distance correspondingly [see Fig. 4(f); the dashed SIC jumps rightward to the solid one]. If the PCL is increased again, the PP would be below the solid SIC, and 2:1 would be obtained in the original 1:1 region. The above is the dynamical process of hysteresis and bistability.

Therefore, the bistability width depends on the distance that the PP chases up the solid SIC rightward. In Ref. [26] a formula calculating the width W is obtained. The basic idea of the formula is to solve the simple traditional chasing problem:

$$L = \int_{T_{P2:1c}}^{T_{p_{2:1c}}+W} \Delta v dt, \tag{4}$$

where L is the initial distance between the PP and the SIC [labeled L in Fig. 4(f)], $\Delta v = v_{PP} - v_{SIC} = 1 - v_{SIC}$ is the velocity difference between the PP and the SIC, and $T_{p_{2:1c}}$ is the PCL corresponding to $PP_{2:1c}$ in Fig. 4(f).

B. Mechanism of bistability in a paced tissue

The dynamics of tissue is more complex than that of a single cell. Because of coupling, stimulation on a cell in the cable does not function as pulsatile pacing with determined magnitude and duration. Therefore, it is difficult to determine the SIC of a cell and the corresponding PP in tissue, and Eq. (4) cannot be directly applied. However, we can qualitatively calculate the width in tissue. If the SIC is regarded to move at an invariant velocity [it is reasonable because the APD is changed approximately linearly with the PCL in the 2:1 branch; also see Fig. 4(a)], Eq. (4) can be simpler, which becomes

$$W = \frac{L}{\Delta v} = \frac{L}{1 - v_{SIC}}. \tag{5}$$

In approximation L and v_{SIC} can be qualitatively obtained. The initial distance L is approximately determined by the APD (denoted by A in the following formulas) difference between critical 1:1 and 2:1 states, so that it is represented as

$$L = A_{2:1c} - A_{1:1c}. \tag{6}$$

Here critical 1:1 and 2:1 refer to the last steady 1:1 state and first steady 2:1 state as the PCL is decreased continuously. The velocity of the SIC is regarded to be the varying rate of the APD as the PCL is changed. Therefore

$$v_{SIC} = \frac{A_{2:1}(T_{p1}) - A_{2:1}(T_{p2})}{2(T_{p1} - T_{p2})}, \tag{7}$$

where $A_{2:1}(T_{p1})$ and $A_{2:1}(T_{p2})$ are APDs on the 2:1 branch at the PCL equaling T_{p1} and T_{p2}, respectively, and T_{p1} and T_{p2} are any two different pacing periods in the bistability region.

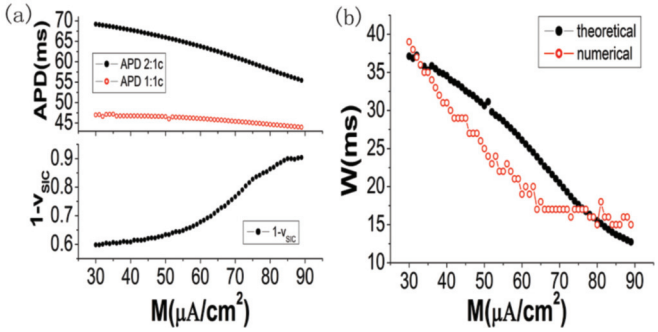

FIG. 5. (Color online) Explanation of the descending tendency of W under pulsatile pacing with $T_{pos} = 10$ ms. Data are taken from the sixth cell in tissue. (a) The upper trace is APDs of the critical 1:1 (red empty circles) and 2:1 (black solid circles) states as functions of pacing magnitude. The lower trace is the velocity difference between PP and SIC (1-v_{SIC}) as a function of magnitude. (b) Comparison of the theoretical and numerical results. Numerical result (empty red circles) is just that shown by Fig. 2(a), and theoretical result comes from Eq. (5). Theoretical result qualitatively fit the numerical one.

Figure 5 is the situation of the sixth cell under pulsatile pacing [form of $R[M(10\text{ ms}),0]$]. Figure 5(a) shows $A_{1:1c}$, $A_{2:1c}$ and $1 - v_{SIC}$ of the cell as functions of pacing magnitude. The black solid circles in Fig. 5(b) are the results obtained from Eq. (5). Theoretical results fit well qualitatively with the numerical ones. The theory provides the descending tendency as that measured numerically, and the order of magnitude of the theoretical result is correct. The reason of the descending tendency of W under pulsatile pacing is that the difference between $A_{1:1c}$ and $A_{2:1c}$ is evidently decreased, and Δv is slightly increased as pacing magnitude is increased.

Figure 6(a) shows the APDs and Δv under sinusoidal pacing (form of $S[M, -M]$). However, W would be decreased if the quantities are substituted into Eqs. (5)–(7), which does not conform with the numerical result. In sinusoidal pacing the movement of the PP may be more complex, which cannot be regarded to be moving horizontally towards the SIC and thus Eq. (5) should be revised. To reveal such a movement, we define the effective magnitude (M_{eff}) of the cell at x yielded by the coupling current from the neighboring cells:

$$M_{\text{eff}} = \frac{1}{t_{up}} \int_0^{t_{up}} D\nabla^2 V_m(x,t)dt. \tag{8}$$

$D\nabla^2 V_m(x,t)$ is the coupling term of point x. About t_{up} demonstrations are given as follows. In the 2:1 state, if one time of stimulus (called S1) successfully elicits an AP in the cable, the stimulus immediately following S1 (called S2) fails to do that. However, S2 still depolarizes the cells adjacent to the paced end. t_{up} is measured during the period that the cell at x is depolarized by S2. Hence, in Eq. (8) t_{up} is the time interval in which $D\nabla^2 V_m(x,t) > 0$ and $\frac{dV_m(x,t)}{dt} > 0$. In such a definition, M_{eff} can be regarded as the stimulating magnitude of the PP.

Interestingly, when the PCL is changed, in pulsatile pacing M_{eff} keeps approximately identical [red empty circles in Fig. 6(b)] so that the PP moves horizontally towards the SIC, while in sinusoidal pacing M_{eff} descends approximately linearly as the PCL is increased [black solid circles in

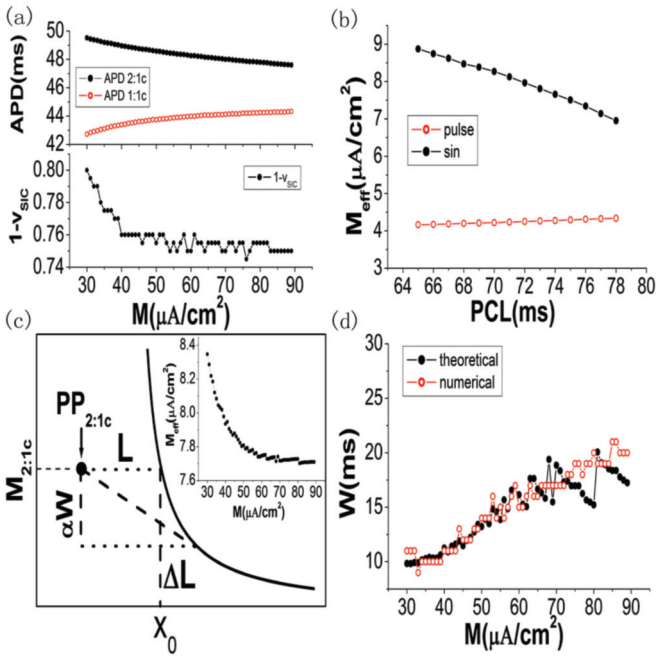

FIG. 6. (Color online) Explanation of the ascending tendency of W under sinusoidal pacing. Data are taken from the sixth cell in tissue. (a) Action potential durations of critical 1:1 and 2:1 states and 1-v_{SIC} as functions of pacing amplitude. (b) Variations of M_{eff} of the sixth cell as PCL is increased under pulsatile (red empty circles) and sinusoidal (black solid circles) pacing, respectively. The pacing magnitudes (amplitudes) are both $50\mu\text{A/cm}^2$. (c) A schematic figure showing the relative movement of PP and SIC under sinusoidal pacing, which leads to Eq. (10) in text. The small frame in the upper right is $M_{2:1c}$ as the function of M. (d) Comparison of the theoretical and numerical results. Numerical result (empty red circles) is just that shown by Fig. 2(a), and theoretical results come from Eq. (10) by setting $C = 1.0$, $E = 6.225$, and $\beta = 1.0$. Theoretical results qualitatively fit the numerical one.

Fig. 6(b)]. When the pacing magnitude is changed, the value of M_{eff} will be changed, but the slope remains nearly invariant. The reduction of M_{eff} in Fig. 6(b) can be interpreted as follows: As the PCL is increased, the functioning time of the hyperpolarizing part is increased, and consequently the cell adjacent to the pacing will be more hyperpolarized. Hence, the coming perturbation (S2) needs more time to depolarize the cell. As M_{eff} is defined to be the time averaged magnitude, it will be decreased. The decrease of M_{eff} is a result of the strengthening of the hyperpolarizing effect. As the distance becomes further from the paced end, the hyperpolarizing effect is "forgotten" by the cable, and the property does not hold. The reduce of M_{eff} can only be seen when $x \leqslant 0.196$ cm (within seven cells from the paced end). As we have already seen that distant cells always follow the adjacent cells to fall in 2:1 and 1:1 states, the characteristic in the region $x \leqslant 0.196$ cm just reveals the difference between pulsatile and sinusoidal pacing.

For sinusoidal pacing, by taking into account the descending movement of M_{eff}, Eq. (5) is revised as follows. First, we conjecture that the SIC can be expressed as $f(x) = Ce^{\beta/x} + E$ [conjectured from Fig. 4(d), where $x \to 0$ means $T_p \to 0$]. The initial positions of the PP and the SIC are shown in Fig. 6(c), which is just a schematic diagram and not created

by actual data. The initial M_{eff} is measured by the critical 2:1 state, and is called $M_{2:1c}$. Suppose the vertical velocity of the PP is α [equal to the slope of the PCL-M_{eff} curve in Fig. 6(b), which is constant despite M variations]. The tilt dashed line represents the trace of the PP movement. That means the PP has to move a larger distance than L to chase up the SIC. Therefore, Eq. (5) should be rewritten as

$$L + \Delta L = \Delta v W. \tag{9}$$

When the PP chases up the SIC, it has taken a distance of αW vertically. In linear approximation, $\Delta L = \alpha W/k$, where k is the slope of the SIC at x_0. So that $k = C\frac{\beta}{x_0^2}e^{\beta/x_0}$, and x_0 satisfies $M_{2:1c} = Ce^{\beta/x_0} + E$. Consequently, $k = \frac{(M_{2:1c}-E)}{\beta}\ln^2(\frac{M_{2:1c}-E}{C})$. Finally, Eq. (9) is rewritten as

$$W = \frac{L}{\Delta v - \frac{\alpha}{\frac{(M_{2:1c}-E)}{\beta}\ln^2(\frac{M_{2:1c}-E}{C})}}. \tag{10}$$

The initial effective magnitude $M_{2:1c}$ as a function of pacing magnitude M is plotted by the small frame in the upper right of Fig. 6(c). If the following values are taken: $\alpha = 0.13$ [measured from Fig. 6(b)], $\beta = 1.0$, $E = 6.225$, and $C = 1$, and by substituting the quantities shown in Figs. 6(a) and 6(c), the results of Eq. (10) qualitatively fit well with those measured numerically, which are shown in Fig. 6(d) by solid black circles. The values of C, E, and β are essentially determined by the shape of the SIC, and the present values are conjectured to fit the results. For different cells, the parameters are different because they are influenced by pacing in different extents. Although the parameters cannot be determined physically in the present study, the revision term in the denominator of Eq. (10) should be the reason for the W ascending under sinusoidal pacing. If $\alpha = 0$, Eq. (10) becomes Eq. (5), which is the formula for pulsatile pacing.

Although the theory provides a qualitative explanation of the width variations, there are quantitative discrepancies between the theoretical and numerical results. The main reasons may be the following: (1) the linear approximation of the theory; (2) a lack of taking into account the spatiotemporal properties of tissue; (3) the simple conjecture of the analytical expression of the SIC and the related parameter values. A more precise theory concerning the quantitative accuracy is awaited.

V. SUMMARY

The present paper investigates the variations of bistability width in periodically paced cardiac tissue as the pacing magnitudes and forms are varied. The following conclusions are obtained:

(i) Pacing forms can be classified into two types: the pulsatile type and the sinusoidal type. In a given form of pacing, as the magnitude (amplitude) is increased, for the pulsatile type, bistability width is decreased while for the sinusoidal type the tendency is the opposite.

(ii) The hyperpolarizing part influences bistability width in a greater extent than the depolarizing part of the pacing. The emergence of the hyperpolarizing part may evidently change the variation tendency of the width. Further increase of the hyperpolarizing ratio in a pacing period transforms the pacing from pulsatile to the sinusoidal type. An increase of the hyperpolarizing ratio can evidently reduce the width. In comparison, the depolarizing part has less effect on the width.

(iii) A theoretical formula is used to calculate the width approximately: $W = L/\Delta v$. The descending of the width under the pulsatile type pacing is due to that L is reduced (i.e., the difference of APDs between critical 1:1 and 2:1 states is reduced), and Δv is increased. However, in sinusoidal pacing, the formula should be revised to be $W = L/(\Delta v - \frac{\alpha}{\frac{(M_{2:1c}-E)}{\beta}\ln^2(\frac{M_{2:1c}-E}{C})})$, which takes into account the factor that effective stimulation magnitude is reduced as the PCL is increased. The revision term in the denominator implies the ascending tendency of width.

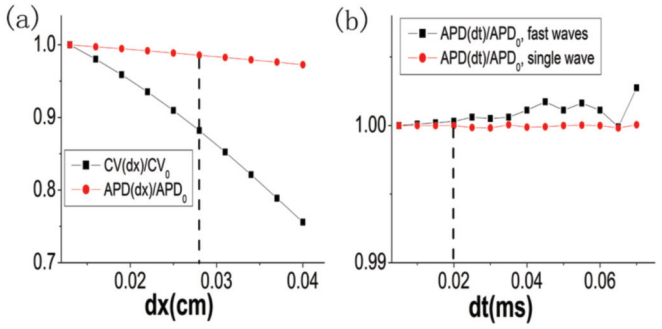

FIG. 7. (Color online) Estimations of numerical errors. The system is paced by pulsatile stimulation with $M = 50(\mu\text{A/cm}^2)$ and duration of 10 ms. The estimations are carried out under 1:1 state of $T_p = 85$ ms. The APD and CV of entrainment are measured on the 150th grid point. APD_0 and CV_0 are APD and CV in the $dt \to 0$ and $dx \to 0$ limits, and the ratio of APD/APD_0 and CV/CV_0 are used to show the error. (a) Errors of APD and CV produced by dx. Conduction velocity is more sensitive than APD to dx. The choice of $dx = 0.028$ cm is indicated by the dashed line, which produces an error of 1.5% in APD and 11% in CV. (b) Errors of APD produced by dt. Two cases are shown: APD of single wave and APD of wave train. Time step dt has little influence on APD in both cases. In $dt = 0.02$ ms, indicated by the dashed line, the error is less than 1%.

ACKNOWLEDGMENTS

This work was supported by the National Natural Science Foundation of China under Grants No. 11205062, No. 11205061, and No. 11105003, and by the Fundamental Research Funds for the Central Universities under Grant No. 105612012ZB0019.

APPENDIX: ERROR ESTIMATIONS OF THE NUMERICAL METHOD

The numerical errors are estimated by varying the spatial and temporal resolutions of dx and dt. The system is paced by pulsatile stimulation with $M = 50(\mu\text{A/cm}^2)$ and duration of 10 ms. The estimations are carried out under the 1:1 state of $T_p = 85$ ms. The APD and conduction velocity (CV) of entrainment are measured on the 150th grid point (which is kept to be far from the paced end as dx is varied). Figures 7(a) and 7(b) are created following the idea of Refs. [31,39]. APD_0 and CV_0 are APD and CV in the $dt \to 0$ and $dx \to 0$ limits. For each dx or dt choice, the ratio of APD/APD_0 and CV/CV_0 is used to show the error.

Figure 7(a) shows the CV and the APD affected by dx. As indicated by Clayton *et al.* [39], the CV is more sensitive than the APD to spatial resolution. The dashed line indicates that dx used in our work ($dx = 0.028$ cm). This choice produces an error of 1.5% in the APD and 11% in the CV. The relatively large error of the CV will not violate the basic properties of bistability. The conduction velocity may influence the propagating block dynamics in cable, but the properties of the APD and the related bistability are little influenced. Figure 7(b) shows the influence of dt. Action potential durations of two cases are measured: the APD of a single wave, and the APD of the wave under overdrive pacing ($T_p = 85$ ms). The error of overdrive pacing is larger than the single wave case. However, in the choice of $dt = 0.02$ ms in the present work (indicated by the dashed line), the error of the APD is less than 1%, which shows that the numerical results are robust to dt.

The numerical errors of the choice of dx and dt in the present work are of an acceptable degree. The robustness of the numerical results indicates that the method can meet the computational needs.

[1] D. P. Zipes and H. J. J. Wellens, Circulation **98**, 2334 (1998).
[2] N. Wessel, J. Kurths, W. Ditto, and R. Bauernschmitt, Chaos **17**, 015101 (2007).
[3] H. Arevalo, B. Rodriguez, and N. Trayanova, Chaos **17**, 015103 (2007).
[4] J. B. Nolasco and R. W. Dahlen, J. Appl. Physiol. **25**, 191 (1968).
[5] J. N. Weiss, A. Karma, Y. Shiferaw, P.-S. Chen, A. Garfinkel, and Z. Qu, Circ. Res. **98**, 1244 (2006).
[6] A. T. Winfree, *When Time Breaks Down* (Princeton University Press, Princeton, NJ 1987).
[7] A. T. Winfree, Science **266**, 1003 (1994).
[8] Z. Qu, J. N. Weiss, and A. Garfinkel, Phys. Rev. E **61**, 727 (2000).
[9] Y. Xie, G. Hu, D. Sato, J. N. Weiss, A. Garfinkel, and Z. Qu, Phys. Rev. Lett. **99**, 118101 (2007).
[10] V. N. Biktashev and A. V. Holden, Proc. R. Soc. London, Ser. B **263**, 1373 (1996).
[11] K. Hall, D. J. Christini, M. Tremblay, J. J. Collins, L. Glass, and J. Billette, Phys. Rev. Lett. **78**, 4518 (1997).
[12] A. T. Stamp, G. V. Osipov, and J. J. Collins, Chaos **12**, 931 (2002).
[13] A. Isomura, M. Horning, K. Agladze, and K. Yoshikawa, Phys. Rev. E **78**, 066216 (2008).
[14] G. R. Mines, J. Physiol. **46**, 349 (1913).
[15] S. Cukierman and A. P. Paes de Carvalho, J. Gen. Physiol. **79**, 1017 (1982).
[16] M. Landau, P. Lorente, and S. C. J. Henry, J. Math. Biol. **25**, 491 (1987).
[17] P. Lorente, C. Delgado, M. Delmar, D. Henzel, and J. Jalife, Circ. Res. **69**, 1301 (1991).
[18] R. Wu and A. Patwardhan, Circ. Res. **94**, 634 (2004).
[19] A. Vinet, D. R. Chialvo, D. C. Michaels, and J. Jalife, Circ. Res. **67**, 1510 (1990).
[20] D. R. Chialvo, D. C. Michaels, and J. Jalife, Circ. Res. **66**, 525 (1990).
[21] M. Delmar, J. Ibarra, P. J. Davidenko, and J. Jalife, Circ. Res. **69**, 1316 (1991).
[22] A. Vinet, J. Biol. Syst. **7**, 451 (1999).
[23] G. M. Hall, S. Bahar, and D. J. Gauthier, Phys. Rev. Lett. **82**, 2995 (1999).
[24] A. R. Yehia, D. Jeandupeux, F. Alonso, and M. R. Guevara, Chaos **9**, 916 (1999).
[25] M. L. Walker, X. Wan, G. E. Kirsch, and D. S. Rosenbaum, Circulation **108**, 2704 (2003).
[26] X. Huang, Y. Qian, X. Zhang, and G. Hu, Phys. Rev. E **81**, 051903 (2010).
[27] F. H. Fenton, E. M. Cherry, H. M. Hastings, and S. J. Evans, Chaos **12**, 852 (2002).
[28] Z. Cao, P. Li, H. Zhang, F. Xie, and G. Hu, Chaos **17**, 015107 (2007).
[29] R. F. Gilmour, Drug Discovery Today **8**, 162 (2003).
[30] C. H. Luo and Y. Rudy, Circ. Res. **68**, 1501 (1991).
[31] M. Hörning, S. Takagi, and K. Yoshikawa, Phys. Rev. E **85**, 061906 (2012).
[32] S. Rush and H. Larsen, IEEE Trans. Biomed. Eng. **25**, 389 (1978).
[33] M. Courtemanche, J. P. Keener, and L. Glass, Siam J. Appl. Math. **56**, 119 (1996).
[34] P. Comtois and A. Vinet, Chaos **12**, 903 (2002).
[35] P. Comtois, A. Vinet, and S. Nattel, Phys. Rev. E **72**, 031919 (2005).
[36] J. M. Anumonwo, M. Delmar, A. Vinet, D. C. Michaels, and J. Jalife, Circ. Res. **68**, 1138 (1991).
[37] H. Hayashi, S.-F. Lin, B. Joung, H. S. Karagueuzian, J. N. Weiss, and P.-S. Chen, Am. J. Physiol. Heart Circ. Physiol. **295**, H1422 (2008).
[38] J. F. Spear and E. N. Moore, Circ. Res. **35**, 782 (1974).
[39] R. Clayton, O. Bernus, E. Cherry, H. Dierckx, F. Fenton, L. Mirabella, A. Panfilov, F. Sachse, G. Seemann, and H. Zhang, Progress Biophys. Mol. Biol. **104**, 22 (2011).